Coupled edge plasmon modes of metal/dielectric multi-wedges*

Wang Xuan-Zhang(王选章)†

Key Laboratory for Photonic and Electronic Band-Gap Materials, National Ministry of Education, and School of Physics and Electronic Engineering, Harbin Normal University, Harbin 150025, China

(Received 25 August 2012; revised manuscript received 24 November 2012)

We present a metallic/dielectric multi-wedge model to investigate the coupled edge plasmon modes (CEPMs), where all wedges have a common edge and the wave propagates along the edge direction. A general theoretical method valid to many practical structures is presented. The analytical dispersion relations of CEPMs in these structures are obtained and the CEPM properties are discussed with numerical results and the dispersion relations. For all structures mentioned in this paper, we find that the structures containing an even number of metallic wedges have four CEPMs and those with an odd-number of metallic wedges have two CEPMs. Further, the periodic structures containing any odd number of periods and any even number of periods possess their common CEPMs, respectively.

Keywords: edge plasmon modes, metallic/dielectric, multi-wedge structures

PACS: 73.20.Mf, 78.20.Ci, 78.20.Bh **DOI:** 10.1088/1674-1056/22/6/067303

1. Introduction

The coupling of the surface or edge plasmons of metals with electromagnetic waves has led to some new optical phenomena and research fields.[1–6] These phenomena possess many potential applications to nano-optics [7] and sub-wavelength optics.[8] The potential applications have aroused great interest in investigating the surface plasmon,[2,9] the edge plasmon,[10–12] and the plasmon polaritons,[2,13] as well as the optical effects of these quasi-particles in various metallic structures in different geometries.[5,6,14,15] We also see other interesting work on the plasmonic optical features of metallic structures.[16,17] Theoretically, numerical simulation methods are often used in a designated geometry to find the properties of the structures when it is very difficult or impossible to obtain analytical results, such as the finite difference time-domain method (FDTD) and vector finite-element method (VFE). For some special metallic/dielectric interfacial structures, such as one-dimensional photonic crystals and superlattices, the analytical results can be found easily.[18] In the electrostatic regime, the surface plasmon (SP) was found at the interface between a metallic film,[2,6] sphere or cylinder[19,20] and a dielectric surrounding, and the edge plasmon was explored around the tip of a metallic wedge.[10,12] The earliest work on discussing the edge modes was presented by Dobrzynski and Maradudin,[21] where they used a single metallic wedge with two planar surfaces, and found two edge plasmon modes, or the symmetrical and anti-symmetrical modes. Subsequently the edge modes of the wedges with the hyperbolic or parabolic cylinder surface were discussed.[11,12] It is well-known that the interaction between electromagnetic waves and the edge plasmons can cause a very high optical localization around the tip of a metallic wedge and it may be very important for the nano-optical and sub-wavelength optical technologies.

We present a multi-wedge model containing metallic wedges to find the dispersion features of coupled edge plasmon modes (CEPMs). Our multi-wedge model is composed of alternate metallic and dielectric wedges, where all wedges have a common edge and the sum of their interior angles is equal to 2π. This model covers many practical situations, such as one single metallic wedge on a dielectric substrate,[22] one metallic bi-wedge in vacuum and on a dielectric substrate,[23] and one dielectric bi-wedge on a metallic substrate.[24]

2. Model and mathematical descriptions

The model is a multi-wedged structure with the cross section as shown in Fig. 1, where the sum of all wedge angles is $\sum_j \alpha_j = 2\pi$ and ε_j indicates the dielectric constant of wedge j. We propose that the wave propagates along the z axis normal to the cross section. In the electrostatic approximation, the potential function of CEPMs in the j-th wedge satisfies the Laplace equation

$$\nabla^2 \phi_j = 0, \tag{1}$$

and the corresponding electric field $\boldsymbol{E}_j = -\nabla\phi_j$. In the cylinder coordinate system, the solution of Eq. (1) is [21]

$$\phi_j = \mathrm{R}(\mu r)(A_j \mathrm{e}^{\mu\theta} + B_j \mathrm{e}^{-\mu\theta})\mathrm{e}^{\mathrm{i}kz}, \tag{2}$$

where k is defined as the wave number, μ is a separated constant and a real number, $\mathrm{R}(\mu r)$ is the modified Bessel function, or the Bessel function of imaginary argument, and decreases

*Project supported by the National Natural Science Foundation of China (Grant No. 11074061) and the Natural Science Foundation of Heilongjiang Province, China (Grant No. ZD200913).

†Corresponding author. E-mail: xzwang696@126.com

© 2013 Chinese Physical Society and IOP Publishing Ltd

as r increases. The boundary conditions of the potential function and the corresponding electric displacement component $D_\theta = \varepsilon E_\theta$ continuous at the interface between two adjacent wedges determine the dispersion relation of CEPMs. As a result, the boundary conditions at the j-th interface lead to the following equations

$$A_j e^{\mu\alpha_j} + B_j e^{-\mu\alpha_j} = A_{j+1} + B_{j+1}, \tag{3a}$$

$$\varepsilon_j(A_j e^{\mu\alpha_j} - B_j e^{-\mu\alpha_j}) = \varepsilon_{j+1}(A_{j+1} - B_{j+1}). \tag{3b}$$

We find a general dispersion equation of CEPMs from these equations,

$$\det\left(\prod_j^N T_j - 1\right) = 0, \tag{4}$$

where det means the determinant of the matrix in the parenthesis, N is the number of interfaces or components in the structure, and T_j is the transform matrix and found from Eq. (3) to be

$$T_j = \frac{1}{2}\begin{pmatrix} \left(1+\dfrac{\varepsilon_j}{\varepsilon_{j+1}}\right)e^{\mu\alpha_j} & \left(1-\dfrac{\varepsilon_j}{\varepsilon_{j+1}}\right)e^{-\mu\alpha_j} \\ \left(1-\dfrac{\varepsilon_j}{\varepsilon_{j+1}}\right)e^{\mu\alpha_j} & \left(1+\dfrac{\varepsilon_j}{\varepsilon_{j+1}}\right)e^{-\mu\alpha_j} \end{pmatrix}. \tag{5}$$

Equations (4) together with Eq. (5) can be used to analytically solve the dispersion relations of CEPMs in many specific structures in the next section. A single metallic wedge in vacuum or in another medium will be first discussed. Although the results in this case have been obtained previously,[21] it is helpful to prove the applicability and correctness of our mathematic description. In this case, the wedge is indicated with subscript 1 and the surrounding medium with 2, dispersion equation (4) is reduced to

$$\det(T_2T_1 - 1) = 2 - 2C_{\alpha_1}C_{\alpha_2} - \Delta_{12}^{+}S_{\alpha_1}S_{\alpha_2} = 0, \tag{6}$$

where there is an additional condition $\alpha_1 + \alpha_2 = 2\pi$, and the simple notions $\Delta_{ij}^{+} = \varepsilon_i/\varepsilon_j + \varepsilon_j/\varepsilon_i$, $C_{\alpha_i} = \cosh(\mu\alpha_i)$, and $S_{\alpha_i} = \sinh(\mu\alpha_i)$ are defined and will be also used in the following sections. Although we do not use the structure symmetry here and equation (6) is different in form from the well-known relations,[21] it can be proven that equation (6) also leads to those known relations. Under the assumptions of $x = \varepsilon_1/\varepsilon_2$ and $y = \mathrm{cth}(\mu\alpha_2/2)\mathrm{th}(\mu\alpha_1/2)$, we easily change Eq. (6) into

$$(y + y^{-1}) = -(x + x^{-1}). \tag{7}$$

It is obvious that there are two solutions,

$$\frac{\varepsilon_1}{\varepsilon_2} = -\mathrm{th}\left(\frac{\mu\alpha_1}{2}\right)\mathrm{cth}\left(\frac{\mu\alpha_2}{2}\right), \tag{8a}$$

$$\frac{\varepsilon_1}{\varepsilon_2} = -\mathrm{cth}\left(\frac{\mu\alpha_1}{2}\right)\mathrm{th}\left(\frac{\mu\alpha_2}{2}\right). \tag{8b}$$

These two solutions are just the symmetric mode and antisymmetric mode obtained with the symmetry analysis in previous work.[21]

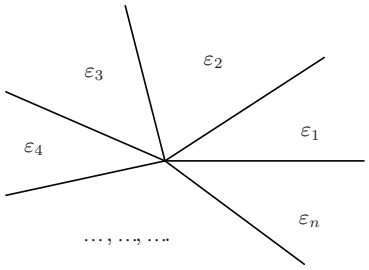


Fig. 1. Cross-section sketch of the model. It is infinite in the z and r directions. We take the cylinder coordinate system and assume the wave to propagate along the z axis (the common edge).

3. Coupled edge plasmons in specific structures

We are interested in such structures, which are easily obtained in practice or possess higher symmetry. Numerical calculations are unavoidable for the structures to be discussed in this section, so some special materials and their physical parameters should be taken. For metallic wedges (or a metallic substrate in a particular structure), the Drude dielectric function[25,26]

$$\varepsilon = \varepsilon_\infty - \frac{(\varepsilon_0 - \varepsilon_\infty)\omega_p^2}{\omega^2} \tag{9}$$

is utilized, with the physical parameters $\varepsilon_\infty = 4.017$, $\varepsilon_0 = 4.896$, and $\omega_p = 1.419 \times 10^{16}$ rad/s from bulk silver.[25,26] We take $\varepsilon_d = 2.3$ for dielectric wedges or a dielectric substrate, which is near to that of SiO_2. Because we consider only dispersion properties of CEPMs in the model, the damping is neglected in the dielectric function of metallic components. In order to clearly analyze the features of CEPMs, we introduce the bulk plasmon frequency $\Omega_{mb} = \omega/\omega_p = 0.468$ corresponding to $\varepsilon = 0$, and the SP frequency of the metal/vacuum interface $\Omega_{mv} = 0.419$ corresponding to $\varepsilon + 1 = 0$ and that of the metal/ dielectric interface $\Omega_{md} = 0.373$ corresponding to $\varepsilon + \varepsilon_d = 0$.

3.1. Structures composed of one wedge and one substrate

A simple structure is composed of one wedge and one semi-infinite substrate in vacuum, where the wedge is placed on the substrate. Three components appear in this structure, i.e., the wedge with dielectric coefficients ε_1, the vacuum with $\varepsilon_2 = 1$ and the substrate with ε_3. The angles satisfy $\alpha_3 = \pi$ and $\alpha_2 = \pi - \alpha_1$. From Eqs. (4) and (5), the dispersion equation of CEPMs is written as an explicit one

$$2C_{\alpha_1}C_{\alpha_2}C_\pi + \Delta_{23}^{+}C_{\alpha_1}S_{\alpha_2}S_\pi + \Delta_{13}^{+}C_{\alpha_2}S_{\alpha_1}S_\pi + \Delta_{12}^{+}C_\pi S_{\alpha_1}S_{\alpha_2} = 2. \tag{10}$$

This equation should be numerically solved to examine dispersion properties of CEPMs. However, there are two interesting cases in this structure, which are valuable to pay close attention to. One is that the wedge is metallic and the substrate is

of dielectric, but the other is opposite to the former, i.e., composed of one dielectric wedge and one metallic substrate.

The numerical results in the first case are illustrated in Fig. 2, where figure 2(a) shows the mode frequencies versus the coefficient μ for various wedge angles and figure 2(b) illustrates the mode frequencies versus wedge angle α_1 for different values of μ. The two modes appear in this case, e.g., the high-frequency mode with the limit value $\Omega_{\rm mv}$, and the low-frequency mode with the limit frequency $\Omega_{\rm md}$. The frequency of high-frequency mode decreases with the increase of μ for smaller values of α_1, but increases for larger values of α_1. The frequency of the low-frequency mode rises as μ increases. The α_1 dependences of mode frequencies for different values of μ show that the frequency of the low-frequency mode increases with α_1 increasing and gradually tends to the limit value $\Omega_{\rm md}$. All curves of the high-frequency mode intersect at the point ($\alpha_1 \approx 2\pi/3$, $\Omega_{\rm mv}$). It is proven that there is such a wedge angle that the CEPM frequency is independent of the coefficient μ and equal to the SP frequency of the metal/vacuum interface. The high-frequency mode monotonically declines in frequency as α_1 increases, and finally reaches its minimum the same as the maximum of the low-frequency mode. The high-frequency and low-frequency modes do not exist at the limit of $\alpha_1 = 0$ and this point also can be found from Eq. (12). In fact, no surface plasmon can appear at the interface between two insulating dielectrics.

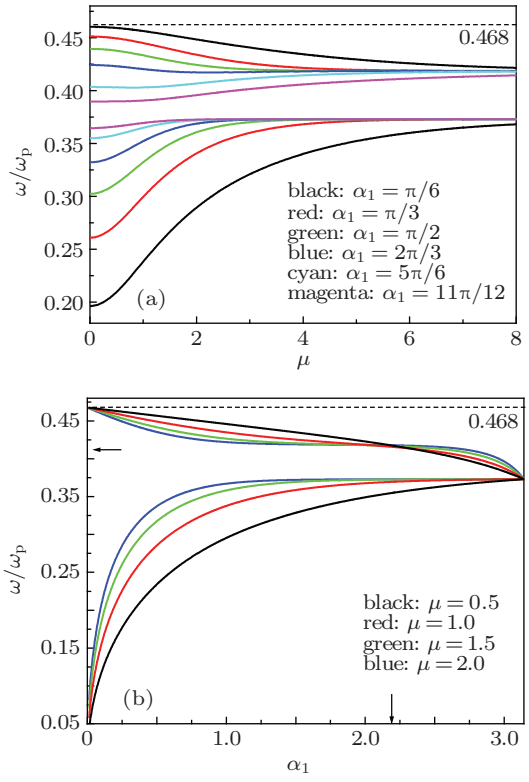


Fig. 2. (color online) Edge plasmons of one metallic wedge on the dielectric substrate, showing (a) mode frequencies versus separated constant μ and (b) versus wedge angle α_1. The arrows point to the coordinates of the intersection position in panel (b).

In the other case, the numerical results are shown in Fig. 3. We first discuss the μ dependence of mode frequency for various wedge angles as illustrated in Fig. 3(a). We see that the two CEPMs are situated in the range between the two surface plasmons, i.e., $\Omega_{\rm mv}$ and $\Omega_{\rm md}$. It is different from Fig. 2(a), where they are situated outside the range, except the high frequency mode in particular conditions. We also present the frequencies versus wedge angle α_1 for different values of μ as shown in Fig. 3(b). This system is obviously different from that in the first case. The two CEPMs possess the same frequency $\Omega_{\rm mv}$ or $\Omega_{\rm md}$, for $\alpha_1 = 0$ or π. In fact, the structure in the case of $\alpha_1 = 0$ or π corresponds to just the metal/vacuum or metal/dielectric interfaces. The high- and low-frequency modes both decrease in frequency as the wedge angle α_1 increases.

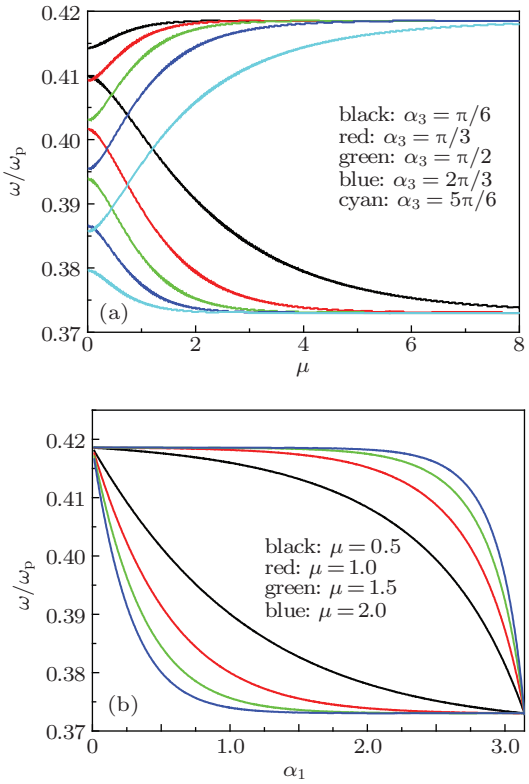


Fig. 3. (color online) Edge plasmons of one dielectric wedge on the metallic substrate, showing (a) mode frequencies versus separated constant μ and (b) versus wedge angle α_1. The two ends of curves in panel (b) correspond to the two SP frequencies, $\Omega_{\rm mv}$ and $\Omega_{\rm md}$.

3.2. Four-component structures with two identical wedges

Structures including two identical metallic wedges or two identical dielectric wedges are also interesting. In this case, equation (4) becomes

$$\det(T_4T_3T_2T_1 - 1) = 0. \tag{11}$$

Here, there are many specific structures to be discussed, which are the structures in the vacuum as follows: the metallic bi-wedge, metallic bi-wedge on a dielectric substrate, and dielectric bi-wedge on a metallic substrate. There generally are

four components in these structures, and we take $\alpha_1 = \alpha_3 = \alpha$ and $\varepsilon_1 = \varepsilon_3 = \varepsilon$ for two identical wedges. α_2 and $\varepsilon_2 = 1$ correspond to the vacuum component. After doing some algebra calculations, equation (11) is written as an explicit dispersion equation as follows:

$$(4C_{\alpha_2}C_{\alpha_4} + \Delta_{21}^{+}\Delta_{41}^{+}S_{\alpha_2}S_{\alpha_4})C_{2\alpha} + 2(\Delta_{21}^{+}S_{\alpha_2}C_{\alpha_4} + \Delta_{41} + S_{\alpha_4}C_{\alpha_2})S_{2\alpha} - \Delta_{21}^{-}\Delta_{41}^{-}S_{\alpha_2}S_{\alpha_4} = 4, \quad (12)$$

where $\Delta_{ij} = \varepsilon_i/\varepsilon_j - \varepsilon_j/\varepsilon_i$ and Δ_{ij}^{+} has been defined above.

We first consider the structure composed of two identical metallic wedges in vacuum, where $\varepsilon_2 = \varepsilon_4 = 1$, so dispersion relation (12) is reduced to

$$2C_{\alpha_2+\alpha_4} + [4C_{\alpha_2}C_{\alpha_4} + (\Delta_{21}^{+})^2 S_{\alpha_2}S_{\alpha_4}]S_{\alpha}^2 + \Delta_{21}^{+}S_{\alpha_2+\alpha_4}S_{2\alpha} = 2. \quad (13)$$

It can be naturally used to discuss dispersion properties of CEPMs in the metallic bi-wedge structure in vacuum. The most interesting case is $\alpha_2 = \alpha_4 = \alpha'$ that corresponds to the highest symmetric structure (or the opposite-wedge structure). A simple dispersion equation is found from $\det[(T_2T_1)^2 - 1]$ to be

$$(\Delta_{21}^{+}S_{\alpha}S'_{\alpha} + 2C_{\alpha}C'_{\alpha})^2 - 4 = 0. \quad (14)$$

Simulating the process of looking for Eq. (8), we discover that this equation possesses four analytical solutions, i.e.,

$$\varepsilon = -\frac{\mathrm{th}(\mu\alpha/2)}{\mathrm{th}(\mu\alpha'/2)}, \quad (15a)$$

$$\varepsilon = -\frac{\mathrm{th}(\mu\alpha'/2)}{\mathrm{th}(\mu\alpha/2)}, \quad (15b)$$

$$\varepsilon = -\mathrm{th}(\mu\alpha/2)\mathrm{th}(\mu\alpha'/2), \quad (15c)$$

$$\varepsilon = -\frac{1}{\mathrm{th}(\mu\alpha/2)\mathrm{th}(\mu\alpha'/2)} \quad (15d)$$

with the constraint condition $\alpha + \alpha' = \pi$. The former two are completely identical to those of a single metallic wedge in vacuum, and are symmetric and asymmetric modes, respectively. An interesting result is that these two modes degenerate into the surface plasmon localized at the metal/vacuum interface as the metallic-wedge angle is equal to $\pi/2$. The latter two are new and should be called mixed-symmetry modes, or symmetric/anti-symmetric modes. For such a structure, there are two reflection symmetric planes at $\alpha/2$ and $\alpha'/2$, respectively. Solution (15c) corresponds to that the potential function in the metallic wedges is symmetrical and the function in vacuum is anti-symmetrical. Solution (15d) is completely opposite to solution (15c). Thus the four modes are related to four possible symmetries. The numerical results are shown in Fig. 4(a). We further see that the top mode related to Eq. (15c) starts in frequency from the bulk plasmon ($\varepsilon = 0$), but the bottom mode corresponding to Eq. (15d) starts from 0-frequency ($\varepsilon \to -\infty$). For $\mu \to \infty$, all modes have the same limit frequency, the SP frequency Ω_{md}. This model can also be used to determine the influence of angle α_2 between the two metallic wedges on the CEPMs. We numerically calculate dispersion relation (12) for $\alpha_1 = \pi/6$ and then the obtained results are illustrated in Fig. 4(b). We can clearly see the effects of changing this angle on the CEPMs.

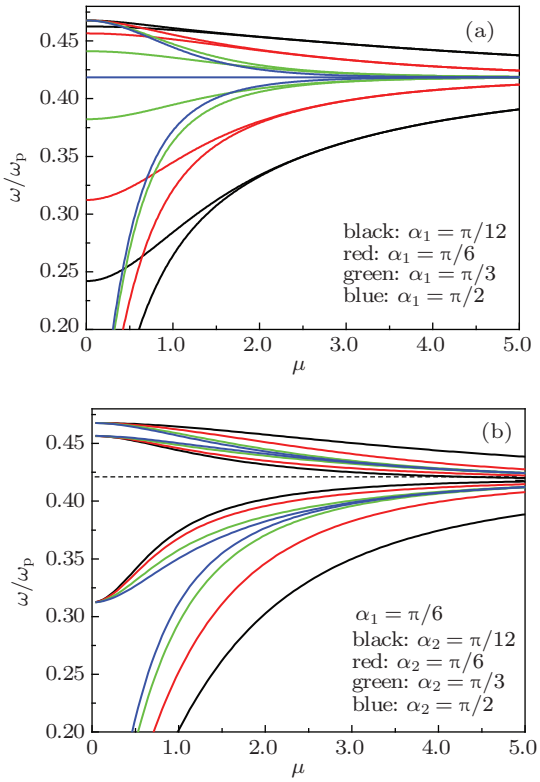


Fig. 4. (color online) Dispersion curves of four coupled edge plasmon modes of a metallic bi-wedge in vacuum, showing (a) the opposite bi-wedge for various wedge angles and (b) the effect of the angle between two metallic wedges on the CEPMs.

We subsequently discuss the structure of two identical metallic wedges on the dielectric substrate, where we take $\alpha_4 = \pi$ and $\varepsilon_4 = 2.3$ in dispersion relation (12). Figure 5(a) shows the numerical results. Comparing these modes with those of the metallic bi-wedge in vacuum shown in Fig. 4(a), the four coupled edge-modes are similar to those in the region of small μ, but they are divided into two groups in the range of large μ, and each group has an individual limit frequency Ω_{mv} or Ω_{md}. We finally discuss such a structure, in which the dielectric bi-wedge is placed on the metallic substrate, with $\alpha_4 = \pi$ and $\varepsilon_1 = 2.3$ in Eq. (12). This structure is opposite to the previous structure and we find only two coupled edge modes as illustrated in Fig. 5(b). The two modes are similar in feature, and both decrease in frequency and tend to the same limit Ω_{md} as μ is enlarged.

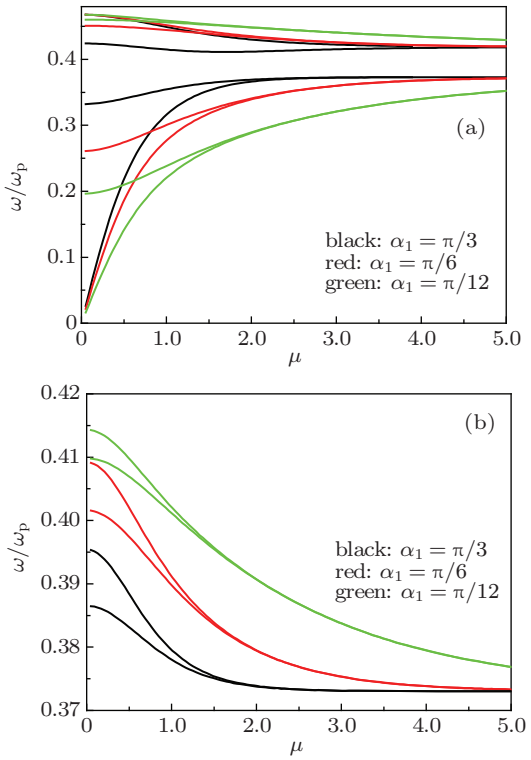


Fig. 5. (color online) Dispersion curves of coupled edge plasmon modes of one bi-wedge on a substrate, showing (a) the metallic bi-wedge on the dielectric substrate and (b) the dielectric bi-wedge on the metallic substrate.

3.3. Periodically metallic/dielectric wedge structures

The last specific systems we are interested in are the periodic structures composed of alternate metallic wedges and dielectric wedges. We denote the metallic wedges with wedge angle α and dielectric constant with ε, and the dielectric wedges with α' and ε'. The period of these structures is $\alpha+\alpha'$ and n represents the period number, so there is the constraint condition of wedge angles, $\alpha+\alpha' = 2\pi/n$. The specific dispersion relation of CEPMs for each given value of n can be obtained from

$$\det(\Lambda^n - 1) = 0, \tag{16}$$

with the matrix

$$\begin{aligned}\Lambda &= T_2 T_1 \\ &= \frac{1}{2}\begin{pmatrix} (2C_{\alpha'} + \Delta^+ S_{\alpha'})\,\mathrm{e}^{\mu\alpha} & -\Delta^- S_{\alpha'}\,\mathrm{e}^{-\mu\alpha} \\ \Delta^- S_{\alpha'}\,\mathrm{e}^{\mu\alpha} & (2C_{\alpha'} - \Delta^+ S_{\alpha'})\,\mathrm{e}^{-\mu\alpha} \end{pmatrix}. \end{aligned} \tag{17}$$

Here, $\Delta^+ = \varepsilon\varepsilon'^{-1} + \varepsilon'\varepsilon^{-1}$ and $\Delta^- = \varepsilon'\varepsilon^{-1} - \varepsilon\varepsilon'^{-1}$. For numerical calculations in this subsection, we take $\varepsilon' = 1$. The 1-period ($n = 1$) and 2-period ($n = 2$) structures are just the single metallic wedge and the opposite-wedge structure, respectively, and have been discussed. For the 3-period structure and 5-period structure, relation (16) can be rewritten as

$$\det(\Lambda - 1)\det(\Lambda^2 + \Delta + 1) = 0, \tag{18a}$$

$$\det(\Lambda - 1)\det(\Lambda^4 + \Lambda^3 + \Lambda^2 + \Lambda + 1) = 0. \tag{18b}$$

The solutions of $\det(\Lambda - 1) = 0$ are just the two modes of the single metallic wedge, except the constraint condition $\alpha + \alpha' = 2\pi/n$. The relations $\det(\Lambda^2 + 1) = 0$ and $\det(\Lambda^4 + \Lambda^3 + \Lambda^2 + \Lambda + 1) = 0$ are analytically expressed as

$$A^2 + B^2 = 0, \tag{19a}$$

$$(A+B)^4 + (A+B)^3 - 3(A+B)^2 - 2(A+B) - 1 = 0, \tag{19b}$$

with $A = 2C_\alpha C'_\alpha \geq 2$ and $B = \Delta^+ S_\alpha S'_\alpha$. Obviously equation (19a) does not own any real solution. Although we cannot directly obtain any conclusion from Eq. (19b), the numerical calculation is used to look for its solutions. As a result, no solution is found in an available frequency range ($0 < \omega/\omega_p < 15.0$). Thus we conclude that the single metallic wedge, 3-period and 5-period structures possess their common CEPMs expressed by Eq. (8), except the constraint condition ($\alpha_1 + \alpha_2 = 2\pi/n$).

Subsequently we discuss the 4-period and 6-period structures. The equations $\det(\Lambda^4 - 1) = 0$ and $\det(\Lambda^6 - 1) = 0$ can be changed into,

$$\det(\Lambda^2 - 1)\det(\Lambda^2 + 1) = 0, \tag{20a}$$

$$\det(\Lambda^2 - 1)\det(\Lambda^2 + \Lambda + 1)\det(\Lambda^2 - \Lambda + 1) = 0. \tag{20b}$$

Here, the solutions of equation $\det(\Lambda^2 - 1) = 0$ have been discussed in Subsection 3.2 and the corresponding CEPMs are just those found from the opposite-wedge structure, or the four CEPMs explicitly shown by dispersion relations (15). However, we should also note that the constraint conditions are different for different period structures. Equation $\det(\Lambda^2 + 1) = 0$ has also been discussed and no solution is found. The equations $\det(\Lambda^2 + \Lambda + 1) = 0$ and $\det(\Lambda^2 - \Lambda + 1) = 0$ can be further written as

$$(A+1)^2 + (B+1)^2 - 1 = 0, \tag{21a}$$

$$(A-1)^2 + (B-1)^2 - 1 = 0. \tag{21b}$$

Due to $A \geq 2$, they do not possess any real solution, so the periodic structures with $n = 2, 4, 6$ have dentical CEPMs, except the constraint condition.

We think that the above conclusions should be extended to periodic structures containing any number of periods. It means that the structures with an odd number of periods have two common CEPMs and those with an even number of periods possess four common CEPMs, except that the constraint conditions are different for different period numbers.

4. Summary and conclusions

We investigate the coupled edge plasmons in the metallic/dielectric multi-wedge structures, where all wedges have a common edge and the sum of wedge angles is equal to 2π.

We first present a general mathematical description of coupled edge plasmon modes (CEPMs) with their field components continuous at interfaces, and then discuss the properties of CEPMs in some typical and specific structures. The physical parameters of metallic components in numerical calculations come from silver, but the dielectric constants of non-metallic components are $\varepsilon = 1$ (vacuum) and $\varepsilon = 2.3$ (SiO_2). We numerically and analytically calculate dispersion relations of CEPMs in the following specific structures, or one metallic (or dielectric) wedge on a dielectric (or metallic) substrate, one metallic (or dielectric) bi-wedge on a dielectric (or metallic) substrate, the opposite metallic bi-wedge in vacuum, and periodical metallic/dielectric structures. We find that the systems containing an odd number of metallic wedges have two CEPMs, but those containing an even number of metallic wedges offer four CEPMs. Further the periodic structures with an odd number of metallic wedges have two common CEPMs, and those with an even number of metallic wedges possess four common CEPMs, except that the constraint condition is different. The two coupled edge modes of the bi-wedge structure given by Eqs. 15(a) and 15(b) were previously calculated within the complete electromagnetic theory,[27] but the two modes described by Eqs. 15(c) and 15(d) are new and they have not been known previously.

Although we neglected the retarded term in the Maxwell equations and adopted the electrostatic approximation in this paper, the obtained results are still interesting since plasmons in metals are in slow electronic oscillation and the plasmon modes are important references of plasmon polaritons. It has been proven that the plasmon mode determined with the electrostatic approximation is only slightly different in frequency from the plasmon polariton described with the complete electromagnetic theory.[10]

References

[1] Martin Dressel and Geoge Gruner 2002 *Electrodynamics of Solids: Optical Properties Of Electrons in Matter* (Cambridge: Cambridge University Press) pp. 71–135

[2] Pitarke J M, Silkin V M, Chulkov E V and Echenique P M 2007 *Rep. Prog. Phys.* **70** 1

[3] Ghaemi H F, Thio T, Grupp D E, Ebbesen T W and Lezec H J 1998 *Phys. Rev. B* **58** 6779

[4] Hutter E and Fendler J H 2004 *Adv. Mater.* **19** 1685

[5] Kim S, Jin J, Kim Y J, Park I Y, Kim Y and Kim S W 2008 *Nature* **453** 757

[6] Safarov V I, Kosobukin V A, Hermann C, Lampel G, Peretti J and Marliere C 1994 *Phys. Rev. Lett.* **73** 3584

[7] Brongersma M L and Kik P G 2007 *Surface Plasmon Nanophotonics* (Springer Series in Optical Sciences) (Springer Dordrecht: The Netherlands)

[8] Barnes W L, Dereux A and Ebbesen T W 2003 *Nature* **424** 824

[9] Orfanides P and Buckner T F 2000 *Am. J. Phys.* **68** 936

[10] Boardman A D, Aers G C and Teshima R 1981 *Phys. Rev. B* **24** 5703

[11] Boardman A D, Garcia-Molina R, Gras-Marti A and Louis E 1985 *Phys. Rev. B* **32** 6045

[12] Garcia-Molina R, Gras-Marti A and Ritchie R H 1985 *Phys. Rev. B* **31** 121

[13] Moreno E, Rodrigo S G, Bozhevolnyi S I, Martin-Moreno L and Garcia-Vidal F J 2008 *Phys. Rev. Lett.* **100** 023901

[14] Ye Y H, Cao Y, Wang Z B, Yan D and Zhang J Y 2009 *Appl. Phys. Lett.* **94** 081118

[15] Barnes W L, Murray W A, Dintinger J, Devaux E and Ebbesen T W 2004 *Phys. Rev. Lett.* **92** 107401

[16] Xie W C, Liu D M and Yang X Y 2008 *Chin. Phys. Lett.* **25** 148

[17] Zhang C L, Ren X F, Huang Y F, Duan K M and Guo G C 2008 *Chin. Phys. Lett.* **25** 559

[18] Cottam M G and Tilley D R 2005 *Introduction to Surface and Superlattice Excitations* (Bristol: Institute of Physics Publishing)

[19] Schroter U 2001 *Phys. Rev. B* **64** 125420

[20] Dasgupta B B 1977 *Zeitschrift Fur Physik B: Conden. Matter* **27** 75

[21] Dobrzynski L and Maradudin A A 1972 *Phys. Rev. B* **6** 3810

[22] Gu L, Sigle W, Koch C T, Ogut B, van Aken P A, Talebi N, Vogelgesang R, Mu J, Wen X and Mao J 2011 *Phys. Rev. B* **83** 195433

[23] Verhagen E, Kuipers L and Polman A 2010 *Nano Lett.* **10** 3665

[24] Haraguchi M, Pile D F P, Okamoto T, Fukui M and Gramotnev D K 2006 *Opt. Rev.* **14** 228

[25] Yan M and Qiu M 2007 *J. Opt. Soc. Am. B* **24** 2333

[26] Palik E D 1985 *Handbook of Optical Constants of Solids, Part II* (Orlando: Academic Press) Subpart 1

[27] Pile D F P, Gramotnev D K, Haraguchi M, Okamoto T and Fukui M 2006 *J. Appl. Phys.* **100** 013101